



Application of ICC LPV control to a blended-wing-body airplane with guaranteed \mathcal{H}_∞ performance



Tianyi He^a, Ali K. Al-Jiboory^a, Guoming G. Zhu^{a,*}, Sean S.-M. Swei^b, Weihua Su^c

^a Department of Mechanical Engineering, Michigan State University, East Lansing, MI, 48823, USA

^b Intelligent Systems Division, NASA Ames Research Center, Moffett Field, CA, 94035, USA

^c Department of Aerospace Engineering and Mechanics, University of Alabama, Tuscaloosa, AL, 35487, USA

ARTICLE INFO

Article history:

Received 15 October 2017

Received in revised form 11 May 2018

Accepted 26 July 2018

Available online 31 July 2018

ABSTRACT

This paper addresses the Input Covariance Constraint (ICC) control problem with guaranteed \mathcal{H}_∞ performance for continuous-time Linear Parameter-Varying (LPV) systems. The upper bound of the output covariance is minimized subject to the constraints on input covariance and \mathcal{H}_∞ output performance. This problem is an extension of the mixed $\mathcal{H}_2/\mathcal{H}_\infty$ LPV control problem, in that the resulting gain-scheduling controllers guarantee not only closed-loop system robustness in terms of \mathcal{H}_∞ norm bound but also output covariance performance over the entire scheduling parameter space. It can be shown that this problem can be efficiently solved by utilizing the convex optimization of Parameterized Linear Matrix Inequalities (PLMIs). The main contributions of this paper are to characterize the mixed ICC/ \mathcal{H}_∞ LPV control problem using PLMIs and to develop the optimal state-feedback gain-scheduling controllers, while satisfying both input covariance and \mathcal{H}_∞ constraints. The effectiveness of the proposed control scheme is demonstrated through vibration suppression of a blended-wing-body airplane model.

© 2018 Elsevier Masson SAS. All rights reserved.

1. Introduction

Linear Parameter-Varying (LPV) modeling and control have gained significant interest from the control community over the past two decades [1–4]. The main benefit of LPV control is that the varying nature of system dynamics can be captured by the LPV model with its linear system matrices dependent on scheduling parameter. LPV controllers can be designed with its gain scheduled based on scheduling parameters measured in real-time.

A systematic LPV modeling approach was proposed in our previous publication [5,6] for developing reduced-order LPV models for flexible aerospace structures. The sub-sequential LPV control design based on developed LPV models is presented in this article. The mainstream approach of LPV gain-scheduling control design is to formulate control synthesis conditions in terms of Linear Matrix Inequalities (LMIs) or Parameterized Linear Matrix Inequalities (PLMIs) [1,7,8]. Numerically tractable optimization methods, such as convex optimization, can then be applied to solve for feasible or optimal LPV gain-scheduling controllers. LPV control designs with guaranteed \mathcal{H}_2 and/or \mathcal{H}_∞ performance have been

intensively studied in the literature [9–12]. However, in practical aerospace structural control applications, control inputs are often hard-constrained and modeling error is unavoidable. Therefore, how to achieve optimal output performance when subject to constrained control input and bounded modeling error is a critical control design problem, but conventional LPV control design technique cannot handle such a design problem. Therefore, mixed Input Covariance Constraint (ICC) and \mathcal{H}_∞ LPV control is proposed in this paper to deal with this multi-objective optimal control problem.

As an extension of \mathcal{H}_2 control, the ICC control problem is to minimize the output covariance performance subject to the multiple constraints on input covariance. The ICC control plays an especially important role for systems with hard constraints on control authority [13,14]. In practical applications, actuators are utilized to drive the mechanical systems to achieve desired output performance, and these actuators typically have limited capacity. Therefore, it is critical to incorporate these actuator constraints during control design, however, this has not been considered in the traditional LPV control formulation. In addition, the existing optimization formulation for conventional LPV controller design often leads to high-gain controllers, due to the optima-seeking nature of the optimization process. These high-gain controllers would inevitably tend to drive the actuators beyond their physical limitations and could also degrade or even destabilize closed-loop systems [15]

* Corresponding author.

E-mail addresses: hetiany2@egr.msu.edu (T. He), aljiboor@egr.msu.edu (A.K. Al-Jiboory), zhug@egr.msu.edu (G.G. Zhu), sean.s.swei@nasa.gov (S.S.-M. Swei), suw@eng.ua.edu (W. Su).

when the modeling error becomes significant. Furthermore, for multiple exogenous input scenarios, the problem of LPV control design to achieve the best possible performance is still an open research problem.

The dual of ICC problem is the Output Covariance Constraint (OCC) control problem, which is to minimize the control input covariance subject to the constraints on output covariance. Both ICC and OCC control problems for linear systems have been studied extensively in the past. For instance, a linear quadratic control problem minimizing control energy subject to output covariance constraints was first considered in Hsieh et al. [16]. In Zhu et al. [17] an algorithm with guaranteed convergence was proposed, in which the OCC problem was solved by optimally selecting the output weighting matrix and solving the Riccati equation iteratively. After the LMI technique was introduced, both ICC and OCC problems have subsequently been converted into the convex optimization problems with LMI constraints [18,19], and they were solved using convex optimization tools. Al-Jiboory et al. [19] utilized the linear time-invariant (LTI) ICC control design approach to optimize the system performance, in terms of output covariance with given actuator constraints, for both state and output feedback cases. An application of the control synthesis LMI conditions can be found in Al-Jiboory et al. [18]. It should be emphasized that the OCC and ICC control problems mentioned above were all for LTI systems, and only a single \mathcal{H}_2 performance constraint was considered. In other words, there was no guaranteed robust performance for closed-loop systems when subject to modeling errors.

To meet multiple performance requirements, a mixed $\mathcal{H}_2/\mathcal{H}_\infty$ LPV control strategy has been proposed with two separate performance channels for \mathcal{H}_2 and \mathcal{H}_∞ performance specifications. Scherer et al. [20] formulated an $\mathcal{H}_2/\mathcal{H}_\infty$ problem for LPV systems and provided the associated solution by solving the algebraic LMIs. In Scherer et al. [21] a solution to the output-feedback mixed $\mathcal{H}_2/\mathcal{H}_\infty$ LPV control problem was presented. Apkarian et al. [22] developed a tractable and practical LMI formulation for the multi-objective LPV control problem using Linear Fractional Transformation (LFT) representations. All these studies treat the mixed performance control problem without including control input and output performance constraints. Recently, White et al. [3,23] formulated PLMI conditions to solve this multi-objective problem for polytopic discrete-time LPV systems, and provided a solution that guarantees \mathcal{L}_2 to \mathcal{L}_∞ gain and performance. Zhang et al. [24] designed a multi-objective LPV controller for an electronic throttle, and showed that the multi-objective LPV controller is able to improve closed-loop system performance over the baseline PID controller.

The primary objective of this paper is to formulate the continuous-time mixed ICC and \mathcal{H}_∞ control problem by utilizing PLMIs for the state-feedback case. To the best of authors' knowledge, the gain-scheduling state-feedback robust ICC problem with guaranteed \mathcal{H}_∞ performance for continuous-time LPV systems has never been explored in the past. One of the great advantages of the proposed approach is that it provides an effective way of designing a family of LPV controllers with varying gains, allowing to tune the controller gains for LPV systems, which is a capability of great practical significance. To illustrate the benefits of the proposed approach, a blended-wing-body airplane model is considered for vibration suppression. Although a full state-feedback controller has limited practical application, nonetheless it serves as a good basis for formulating the dynamic output feedback controllers.

The rest of paper is organized as follows. Section 2 formulates the mixed ICC and \mathcal{H}_∞ (or robust ICC) control problem, and Section 3 provides LPV modeling of linear systems and introduces affine to multi-simplex transformation. Then, the control synthesis conditions in terms of PLMIs are provided in Section 4, and the

numerical simulations for the blended-wing-body model are conducted in Section 5. The conclusions are in Section 6.

2. Problem formulation

Consider the following affine LPV systems,

$$\Sigma(\theta) : \begin{cases} \dot{x}(t) = A(\theta(t))x(t) + B_\infty(\theta(t))w_\infty(t) \\ \quad + B_2(\theta(t))w_2(t) + B_u(\theta(t))u(t) \\ z_\infty(t) = C_\infty(\theta(t))x(t) + D_\infty(\theta(t))w_\infty(t) \\ \quad + E_\infty(\theta(t))u(t) \\ z_2(t) = C_2(\theta(t))x(t) \end{cases} \quad (1)$$

where $\theta(t) = [\theta_1(t), \theta_2(t), \dots, \theta_q(t)]^T$ denotes the scheduling parameter vector of q elements, $x(t) \in R^{n_x}$ denotes the state, $w_\infty(t) \in R^{n_{w_\infty}}$ the \mathcal{H}_∞ disturbance input due to modeling error, $w_2(t) \in R^{n_{w_2}}$ the \mathcal{H}_2 disturbance input, $u(t) \in R^{n_u}$ the control input, $z_\infty(t) \in R^{n_{z_\infty}}$ the \mathcal{H}_∞ controlled output, and $z_2(t) \in R^{n_{z_2}}$ the \mathcal{H}_2 performance output. All system matrices are assumed to have compatible dimensions and in affine parameter-dependent form. For example, $A(\theta)$ can be described by

$$A(\theta(t)) = A_0 + \sum_{i=1}^q A_i \theta_i, \quad (2)$$

where A_0 and A_i , $i = 1, 2, \dots, q$, are constant matrices. It is assumed that the scheduling parameters are measurable in real-time, and their magnitude and variational rate are bounded. Specifically, the scheduling parameter set is formulated as:

$$\theta \in \Theta = \{\theta_i \leq \theta_i(t) \leq \bar{\theta}_i, -v_{\theta_i} \leq \dot{\theta}_i(t) \leq v_{\theta_i}\}, \quad (3)$$

where $i \in [1, 2, \dots, q]$. In this paper, we propose the gain-scheduling state-feedback controllers of the form

$$u(t) = K(\theta(t))x(t), \quad (4)$$

where $K(\theta)$ is the parameter-dependent control gain matrix. Note that $u(t)$ can be partitioned as $u(t) = [u_1(t), u_2(t), \dots, u_{n_u}(t)]^T$. Then, substituting (4) into (1) yields the closed-loop LPV system described by

$$\Sigma_{cl}(\theta) : \begin{cases} \dot{x}(t) = A_{cl}(\theta)x(t) + B_\infty(\theta)w_\infty(t) + B_2(\theta)w_2(t); \\ z_\infty(t) = C_{cl,\infty}(\theta)x(t) + D_\infty(\theta)w_\infty(t) \\ z_2(t) = C_2(\theta)x(t) \end{cases} \quad (5)$$

where $A_{cl}(\theta) = A(\theta) + B_u(\theta)K(\theta)$, $C_{cl,\infty}(\theta) = C_\infty(\theta) + E_\infty(\theta)K(\theta)$. Throughout this paper, we make use of the following standard definition of \mathcal{L}_2 and \mathcal{L}_∞ norms on $x(t) \in R^n$ for all $t \geq 0$,

$$\|x\|_2^2 := \int_0^\infty x^T(t)x(t)dt, \quad \|x\|_\infty^2 := \sup_{t \geq 0} x(t)^T x(t).$$

2.1. System performance

It should be noted that there are two separate input and output pairs defined in (5), and they are specifically designated for assessing the closed-loop LPV system performances, as shown in Fig. 1. The LPV system $\Sigma(\theta)$ is controlled by the gain-scheduling state-feedback controller (4), to achieve best \mathcal{H}_2 performance while subject to \mathcal{H}_∞ performance requirements and control input constraints. Note that the interconnection of Δ in Fig. 1 is to capture the model uncertainties in $\Sigma(\theta)$. The definitions of \mathcal{H}_∞ and \mathcal{H}_2 performances are given below.

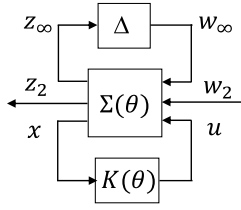


Fig. 1. Closed-loop LPV system with state-feedback control and uncertainty block.

2.1.1. \mathcal{H}_∞ performance

The \mathcal{H}_∞ performance, defined from $w_\infty(t)$ to $z_\infty(t)$ with \mathcal{L}_2 input and \mathcal{L}_2 output, is utilized to assess the closed-loop system robustness in the presence of model uncertainties. Mathematically, let $T_\infty(K(\theta), s) := T_{w_\infty \rightarrow z_\infty}(K(\theta), s)$ denote the transfer function from $w_\infty(t)$ to $z_\infty(t)$, and $\|T_\infty(K(\theta), s)\|_\infty$ the \mathcal{H}_∞ norm of $T_\infty(K(\theta), s)$. Then, the \mathcal{H}_∞ performance for $(w_\infty(t), z_\infty(t))$ pair in (5) is defined as [25]

$$\begin{aligned} \|T_\infty(K(\theta), s)\|_\infty &= \operatorname{ess\,sup}_{\omega \in \mathbb{R}} \bar{\sigma}[T_\infty(K(\theta), j\omega)] \\ &= \sup_{w_\infty, z_\infty \in \mathcal{L}_2, \|w_\infty\|_2 \neq 0} \frac{\|z_\infty(t)\|_2}{\|w_\infty(t)\|_2}. \end{aligned} \quad (6)$$

Physically, \mathcal{H}_∞ norm is related to the robust stability of a given system with modeling error. Based on the Small Gain Theorem [25], the closed-loop system satisfying the condition $\|T_\infty\|_\infty \leq \gamma_\infty$ is well-posed and internally stable for all uncertainty satisfying the constrain $\|\Delta\|_\infty < 1/\gamma_\infty$, where Δ is system uncertain dynamics interconnected from z_∞ to w_∞ , see Fig. 1.

2.1.2. \mathcal{H}_2 performance

Let $T_2(K(\theta), s) := T_{w_2 \rightarrow z_2}(K(\theta), s)$ be the transfer function from $w_2(t)$ to $z_2(t)$, then the \mathcal{H}_2 norm of $T_2(K(\theta), s)$ can be defined by [20]

$$\begin{aligned} \|T_2(K(\theta), s)\|_2^2 &= \sup_{\theta \in \Theta} \frac{1}{2\pi} \int_{-\infty}^{\infty} \operatorname{trace}[T_2^*(K(\theta), j\omega)T_2(K(\theta), j\omega)] d\omega \\ &= \sup_{\theta \in \Theta} \operatorname{trace}(C_2(\theta)\bar{P}_2(\theta)C_2^T(\theta)), \end{aligned} \quad (7)$$

where $\bar{P}_2(\theta)$ is the controllability Gramian solving $\dot{\bar{P}}_2(\theta) + A_{cl}(\theta)\bar{P}_2(\theta) + \bar{P}_2(\theta)A_{cl}(\theta)^T + B_2(\theta)B_2(\theta)^T = 0$.

The \mathcal{H}_2 norm of a system has two interesting physical interpretations both stochastically and deterministically. To be more specific, stochastically, \mathcal{H}_2 norm of a system denotes the trace of the output covariance matrix, or in other words, the summation of RMS-value of the system outputs to a white noise input; and deterministically, \mathcal{H}_2 norm of a system denotes the square summation of \mathcal{L}_2 to \mathcal{L}_∞ gains of individual channels from exogenous disturbance inputs to system outputs. In vibration control, system \mathcal{H}_2 norm can be used as a measure of output magnitude (\mathcal{L}_∞ norm) due to energy limited (\mathcal{L}_2 norm) disturbance inputs.

Note that for LPV control case, $\|T_2(K(\theta), s)\|_2$ depends on varying scheduling parameter θ , leading to increased complexity due to unknown scheduling parameter trajectory. To reduce complexity and keep optimization as a unified approach, the upper bound $\operatorname{trace}(W) \geq \operatorname{trace}(C_2(\theta)\bar{P}_2(\theta)C_2^T(\theta))$ for all θ satisfying (3) is minimized instead. W is an introduced auxiliary variable, which is a symmetric matrix with compatible dimensions with outputs. Using this objective function, the optimal control conditions with guaranteed \mathcal{H}_2 performance for all admissible scheduling parameter are derived, and then, the mixed ICC and \mathcal{H}_∞ control problem can be well formulated in the sequel.

2.2. Mixed ICC and \mathcal{H}_∞ control problem

The mixed ICC and \mathcal{H}_∞ control problem is to find a state-feedback gain-scheduling controller (4) for the LPV system (1), while minimizing the upper bound of \mathcal{H}_2 performance cost

$$\min_{K(\theta)} \operatorname{trace}(W), \quad (8)$$

such that: 1) the closed-loop system (5) is exponentially stable, and 2) the following constraints are satisfied,

$$\|T_\infty(K(\theta), s)\|_\infty \leq \gamma_\infty, \quad (9)$$

$$\operatorname{Cov}(u_k(t)) \leq \bar{U}_k, k = 1, 2, \dots, n_u, \quad (10)$$

where $\gamma_\infty > 0$ is the given \mathcal{H}_∞ -norm bound on system robustness, and \bar{U}_k the given bound on the control covariance $\operatorname{Cov}(u_k(t))$ for the k th control input $u_k(t)$ defined below,

$$\operatorname{Cov}(u_k(t)) = \left[\frac{1}{2\pi} \int_{-\infty}^{\infty} T_u^*(K(\theta), j\omega)T_u(K(\theta), j\omega)d\omega \right], \quad (11)$$

and $T_u(K(\theta), s) := T_{w_2 \rightarrow u}(K(\theta), s)$ denotes the transfer function from $w_2(t)$ to $u(t)$ for the LPV system (5). Note that, for deterministic signal, covariance is defined in terms of time correlation [26].

As a result, the proposed mixed ICC and \mathcal{H}_∞ control problem has interesting interpretations in stochastic and deterministic perspectives. The stochastic interpretation assumes that the exogenous input $w_2(t)$ is an uncorrelated zero-mean white noise with unit intensity. Then, the mixed ICC and \mathcal{H}_∞ control problem is to minimize the output covariance (or RMS-value) while satisfying multiple control input covariance constraints and \mathcal{H}_∞ robust performance criterion. The control input covariance constraints can be considered as constraints on the variances of the control actuation. In other words, the proposed control provides the best output \mathcal{H}_2 performance with the given control \mathcal{H}_2 performance and robust \mathcal{H}_∞ constraints. On the other hand, the deterministic interpretation assumes that the exogenous input $w_2(t)$ is an unknown disturbance that belongs to a bounded \mathcal{L}_2 set. Then, the mixed ICC and \mathcal{H}_∞ control problem is to minimize the square summation of \mathcal{L}_2 to \mathcal{L}_∞ gains from $w_2(t)$ to individual output channel $z_{2,k}(t)$ for $k = 1, 2, \dots, n_{z_2}$, subject to the \mathcal{L}_2 to \mathcal{L}_∞ gain constraints (10) on $u_k(t)$ for $k = 1, 2, \dots, n_u$ and the \mathcal{H}_∞ constraint (9). In other words, the proposed control problem is to minimize the weighted sum of the worst case peak values of performance output subject to the constraints on worst-case peak values of control inputs and the \mathcal{H}_∞ constraint. It should be noted that the \mathcal{L}_2 - \mathcal{L}_∞ gain from $w_2(t)$ to $z_2(t)$ is defined in White et al. [23] as follows,

$$\begin{aligned} \bar{\sigma} \left[\frac{1}{2\pi} \int_{-\infty}^{\infty} T_2^*(K(\theta), j\omega)T_2(K(\theta), j\omega)d\omega \right] &= \sup_{w_2 \in \mathcal{L}_2, z_2 \in \mathcal{L}_\infty, \|w_2\|_2 \neq 0} \frac{\|z_2(t)\|_\infty^2}{\|w_2(t)\|_2^2} \end{aligned} \quad (12)$$

where $\bar{\sigma}[\cdot]$ denotes the maximum singular value operator.

3. Modeling scheduling parameters

The scheduling parameter vector considered in (1) is defined in an affine manifold, so we first need to map that into a multi-simplex manifold for subsequent convex analysis. Following the procedure presented in Lacerda et al. [27] and Oliveira et al. [28], the original parameter domain can be converted into a convex

multi-simplex domain. Note that a multi-simplex domain is defined as the Cartesian product of multiple unit-simplexes. Thus, the scheduling parameter $\theta_i(t)$ can be converted into the unit-simplex variable $\alpha_i(t)$ using the following formula,

$$\alpha_{i,1} = \frac{\theta_i(t) - \underline{\theta}_i}{\bar{\theta}_i - \underline{\theta}_i}, \quad \alpha_{i,2} = 1 - \alpha_{i,1} = \frac{\bar{\theta}_i - \theta_i(t)}{\bar{\theta}_i - \underline{\theta}_i}, \quad i = 1, 2, \dots, q. \quad (13)$$

As a result, we have $\alpha_i = (\alpha_{i,1}, \alpha_{i,2}) \in \Lambda_{i,2}$, where the two dimensional unit-simplex $\Lambda_{i,2}$ for α_i is defined as

$$\Lambda_{i,2} := \{\alpha_i \in \mathbf{R}^2 : \sum_{k=1}^2 \alpha_{i,k} = 1, \alpha_{i,k} \geq 0\}.$$

Hence, the unit-simplex variable $\alpha_i \in \Lambda_{i,2}$ is created. Similarly, the time derivative of the scheduling parameter can also be converted into a unit-simplex variable by utilizing the following condition,

$$\dot{\alpha}_{i,1}(t) + \dot{\alpha}_{i,2}(t) = 0. \quad (14)$$

Hence, the rates of convex parameters are bounded as follows,

$$\frac{-v_{\theta_i}}{\bar{\theta}_i - \underline{\theta}_i} \leq \dot{\alpha}_{i,k} \leq \frac{v_{\theta_i}}{\bar{\theta}_i - \underline{\theta}_i}, \quad i = 1, 2, \dots, q; \quad k = 1, 2. \quad (15)$$

Note that the time derivative of parameter α_i lies in the space modeled by the convex combination of the columns of the matrix $H_i \in \mathbf{R}^{2 \times 2}$ given by

$$H_i = \begin{bmatrix} -\frac{v_{\theta_i}}{\bar{\theta}_i - \underline{\theta}_i} & \frac{v_{\theta_i}}{\bar{\theta}_i - \underline{\theta}_i} \\ \frac{v_{\theta_i}}{\bar{\theta}_i - \underline{\theta}_i} & -\frac{v_{\theta_i}}{\bar{\theta}_i - \underline{\theta}_i} \end{bmatrix}, \quad i = 1, 2, \dots, q, \quad (16)$$

and $\dot{\alpha}_i$ can be established using a unit-simplex of dimension 2 as

$$\Omega_{i,2} := \{\phi_i \in \mathbf{R}^2 : \phi_i = \sum_{k=1}^2 \eta_{i,k} H_i^k, \eta_i \in \Lambda_{i,2}\}, \quad i = 1, 2, \dots, q, \quad (17)$$

where $\eta_i = (\eta_{i,1}, \eta_{i,2})$ and H_i^k denotes the k th column of matrix H_i . Therefore, the unit-simplex variable $\dot{\alpha}_i \in \Omega_{i,2}$ is created. Furthermore, the scheduling parameters $(\theta, \dot{\theta})$ with given bounds can then be converted into multi-simplex domain from Cartesian product of multiple unit-simplexes as follows,

$$(\alpha, \dot{\alpha}) \in \Lambda \times \Omega := \prod_{i=1}^q \Lambda_{i,2} \times \prod_{i=1}^q \Omega_{i,2}.$$

By utilizing the scheduling parameter transformation presented above, the LPV system $\Sigma(\theta)$ described in (1), which is an affine function of parameter θ , can now be transformed into an LPV system representation $\Sigma(\alpha)$ that is a function of α in multi-simplex domain. For simplicity, we assume that $\Sigma(\alpha)$ takes the same form as $\Sigma(\theta)$ in that all the system matrices are now functions of α . Subsequently, the LPV controller design, to be presented in the next section, will be based on the convex scheduling parameter α . However, in actual control implementation, the designed LPV controller in multi-simplex α domain will need to be mapped back to the controller in affine θ domain [28].

4. Controller synthesis PLMIs

This section provides the synthesis PLMI conditions for the proposed mixed ICC and \mathcal{H}_∞ control problem. To make it numerically more tractable, the upper bound of the \mathcal{H}_2 norm, instead of actual \mathcal{H}_2 norm, is minimized. The next theorem contains the main result of this paper.

Theorem 1. Given the input covariance constraints $\bar{U}_k, k = 1, 2, \dots, n_u$, and a positive scalar γ_∞ , if there exist continuously differentiable parameter-dependent matrix $0 < P_2(\alpha) = \bar{P}_2^T(\alpha) \in \mathbf{R}^{n_x \times n_x}$, $0 < P_\infty(\alpha) = \bar{P}_\infty^T(\alpha) \in \mathbf{R}^{n_x \times n_x}$, $G(\alpha) \in \mathbf{R}^{n_x \times n_x}$, $Z(\alpha) \in \mathbf{R}^{n_u \times n_x}$, small scalars $\epsilon_2 > 0$ and $\epsilon_\infty > 0$, and matrix $W = W^T \in \mathbf{R}^{n_{z_2} \times n_{z_2}}$ that minimize the following cost function with a given scaling matrix $Q > 0$,

$$\min \text{trace}(QW) \quad (18)$$

subject to the following inequalities (* denotes symmetric terms),

$$\begin{bmatrix} \Phi_{11} & * & * \\ \Phi_{12} & -\epsilon_2(G(\alpha) + G(\alpha)^T) & * \\ B_2(\alpha)^T & \mathbf{0}_{n_w \times n_w} & -\mathbf{I}_{n_w} \end{bmatrix} < 0, \quad (19)$$

$$\begin{bmatrix} W & C_2(\alpha)G(\alpha) \\ * & G(\alpha) + G(\alpha)^T - P_2(\alpha) \end{bmatrix} > 0, \quad (20)$$

$$\begin{bmatrix} \bar{U}_k & \Psi_k Z(\alpha) \\ * & G(\alpha) + G(\alpha)^T - P_2(\alpha) \end{bmatrix} > 0, \quad k = 1, 2, \dots, n_u, \quad (21)$$

$$\begin{bmatrix} \Phi_{\infty 1} & * & * & * \\ \Phi_{\infty 2} & -\epsilon_\infty(G(\alpha) + G(\alpha)^T) & * & * \\ \Phi_{\infty 3} & \epsilon_\infty \Phi_{\infty 3} & -\mathbf{I}_{n_z} & * \\ B_\infty(\alpha)^T & \mathbf{0}_{n_w \times n_x} & D_\infty(\alpha)^T & -\gamma_\infty^2 \mathbf{I}_{n_w} \end{bmatrix} < 0, \quad (22)$$

where $\Phi_{11} = A(\alpha)G(\alpha) + B_u(\alpha)Z(\alpha) + (A(\alpha)G(\alpha) + B_u(\alpha)Z(\alpha))^T - \frac{\partial P_2(\alpha)}{\partial \alpha} \dot{\alpha}$, $\Phi_{12} = P_2(\alpha) - G(\alpha) + \epsilon_2(A(\alpha)G(\alpha) + B_u(\alpha)Z(\alpha))^T$, and Ψ_k is input channel selection matrix for control input of interest, and $\Phi_{\infty 1} = A(\alpha)G(\alpha) + B_u(\alpha)Z(\alpha) + (A(\alpha)G(\alpha) + B_u(\alpha)Z(\alpha))^T - \frac{\partial P_\infty(\alpha)}{\partial \alpha} \dot{\alpha}$, $\Phi_{\infty 2} = P_\infty(\alpha) - G(\alpha) + \epsilon_\infty(A(\alpha)G(\alpha) + B_u(\alpha)Z(\alpha))^T$, and $\Phi_{\infty 3} = C_\infty(\alpha)G(\alpha) + E_\infty(\alpha)Z(\alpha)$. Then, the gain-scheduling controller

$$u(t) = K(\alpha)x(t), \quad K(\alpha) = Z(\alpha)G^{-1}(\alpha) \quad (23)$$

exponentially stabilizes the LPV system $\Sigma(\alpha)$ for any $(\alpha, \dot{\alpha}) \in \Lambda \times \Omega$ with a guaranteed \mathcal{H}_∞ performance bound γ_∞ . In addition, the ICC cost is bounded by

$$\text{trace}(W) > \text{trace} \left\{ C_2(\alpha)P_2(\alpha)C_2(\alpha)^T \right\}, \quad (24)$$

and the constraint (10) is satisfied.

Proof. For closed-loop LPV system (5), assume $A_{cl}(\alpha)$ is stable for any pair $(\alpha, \dot{\alpha}) \in \Lambda \times \Omega$, then there is a continuously differentiable parameter-dependent positive-definite matrix $\bar{P}_2(\alpha) = \bar{P}_2^T(\alpha) > 0$, such that

$$\dot{\bar{P}}_2(\alpha) + A_{cl}(\alpha)\bar{P}_2(\alpha) + \bar{P}_2(\alpha)A_{cl}(\alpha)^T + B_2(\alpha)B_2(\alpha)^T = 0 \quad (25)$$

where $\bar{P}_2(\alpha)$ is the controllability Gramian of the LPV system. In other words, there is a parameter-dependent positive-definite matrix $P_2(\alpha) > \bar{P}_2(\alpha)$ satisfying the following inequality

$$\dot{P}_2(\alpha) + A_{cl}(\alpha)P_2(\alpha) + P_2(\alpha)A_{cl}(\alpha)^T + B_2(\alpha)B_2(\alpha)^T < 0. \quad (26)$$

To decouple $A_{cl}(\alpha)$ and $P_2(\alpha)$ in (26), we utilize Finsler's Lemma [29] to obtain the following,

$$\Gamma(\alpha) + X(\alpha)V(\alpha) + V^T(\alpha)X^T(\alpha) < 0, \quad (27)$$

where

$$\Gamma(\alpha) = \begin{bmatrix} \dot{P}_2(\alpha) & P_2(\alpha) & 0 \\ P_2(\alpha) & 0 & 0 \\ 0 & 0 & I \end{bmatrix}, \quad X(\alpha) = \begin{bmatrix} G^T(\alpha) & 0 \\ R^T(\alpha) & 0 \\ 0 & I \end{bmatrix}$$

$$V(\alpha) = \begin{bmatrix} A_{cl}^T(\alpha) & -I & 0 \\ B_2^T & 0 & -I \end{bmatrix},$$

and $G(\alpha)$ and $R(\alpha)$ are introduced as slack variables. To maintain convex parametrization property, $R(\alpha)$ is chosen to be $R(\alpha) = \epsilon_2 G(\alpha)$, where $\epsilon_2 > 0$ is a scalar that is used to provide an extra degree-of-freedom when performing the line search and to reduce conservativeness. Letting $Z(\alpha) = K(\alpha)G(\alpha)$ yields (19).

Now, consider (20). Pre- and post-multiplying (20) by $[I, C_2]$ and $[I, C_2]^T$ renders

$$\begin{bmatrix} I & C_2 \end{bmatrix} \begin{bmatrix} W & C_2(\alpha)G(\alpha) \\ * & G(\alpha) + G(\alpha)^T - P_2(\alpha) \end{bmatrix} \begin{bmatrix} I \\ C_2^T \end{bmatrix} > 0 \quad (28)$$

from which we obtain

$$W > C_2(\alpha)P_2(\alpha)C_2(\alpha)^T, \quad (29)$$

hence (29) leads to (24). Since

$$C_2(\alpha)P_2(\alpha)C_2(\alpha)^T > C_2(\alpha)\bar{P}_2(\alpha)C_2(\alpha)^T,$$

as a result, minimizing $\text{trace}(QW)$ implies minimizing the upper bound of the weighted ICC cost.

Similarly, pre- and post-multiplying (21) by $[I, \Psi_k K(\alpha)]$ and $[I, \Psi_k K(\alpha)]^T$ to obtain

$$\begin{bmatrix} I & \Psi_k K(\alpha) \end{bmatrix} \begin{bmatrix} \bar{U}_k & \Psi_k Z(\alpha) \\ * & G(\alpha) + G(\alpha)^T - P_2(\alpha) \end{bmatrix} \begin{bmatrix} I \\ (\Psi_k K(\alpha))^T \end{bmatrix} > 0, \quad (30)$$

which yields

$$\bar{U}_k > \Psi_k K(\alpha)P(\alpha)K(\alpha)^T \Psi_k^T, \quad k = 1, 2, \dots, n_u.$$

This implies that the selected control input covariance is upper bounded by \bar{U}_k .

Now, for \mathcal{H}_∞ performance inequality (22), we consider the following transformation matrix

$$T(\alpha) = \begin{bmatrix} I & A_{cl}(\alpha) & 0 & 0 \\ 0 & C_{cl,\infty}(\alpha) & I & 0 \\ 0 & 0 & 0 & I \end{bmatrix}.$$

Pre- and post-multiplying (22) by $T(\alpha)$ and $T(\alpha)^T$ leads to the \mathcal{H}_∞ performance criterion based upon the well-known *Real Bounded Lemma* [11] that the \mathcal{H}_∞ norm of the closed-loop system is bounded by γ_∞ . This can be easily verified by plugging in search variables and operating matrix multiplication. \square

Remark 1. For each given set of small positive scalar variables ϵ_2 and ϵ_∞ , the minimization leads to a sub-optimal solution. Fixing both scalar variables would lead to conservativeness, however, the line search of scalar variables can reduce conservativeness significantly. Note that constraining $P_\infty = P_2$ for multi-objective control design, as commonly found in the literature, could lead to large conservativeness. The optimization process can be repeated for a set of gridded scalar values to minimize $\text{trace}(QW)$. The line search process may burden the computational load, but with current advanced computational capacity, this should not be an issue.

The formulated PLMIs are equivalent to infinite dimensions of LMIs, and the recent robust synthesis framework provides rigorous method to handle PLMIs [8,28,30]. In this research, the matrix coefficient check relaxation approach [28] has been utilized to solve the developed PLMIs, especially in multi-simplex domain. The algebraic operation for PLMIs can be a challenge, but ROLMIP [31] has been one of the more effective parsers available to specifically handle these PLMIs. This package is based on MATLAB and works jointly with parser YALMIP [32] and solver SeDuMi [33]. In this paper, the optimization problem is solved by utilizing these tools.

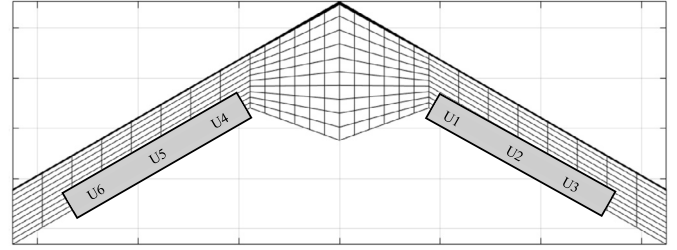


Fig. 2. Schematic diagram of blended-wing-body airplane.

5. Numerical example: blended-wing-body airplane model

To demonstrate that the proposed robust ICC controller is able to achieve control design objectives, the LPV modeling and control of a Blended-Wing-Body (BWB) airplane is considered. The longitudinal dynamics of BWB aero-elastic models were found to be varying with flight speeds in Su and Cesnik [6], therefore in this study the flight speed is considered as the only scheduling parameter θ . The objective of this study is to find a gain-scheduling LPV state-feedback controller to effectively suppress the vibration of BWB airplane wing. The system performance defined in Section 2 can be interpreted in physical terms, where \mathcal{H}_∞ performance is related to the robustness to modeling error and \mathcal{H}_2 performance is associated with the ability to suppress excessive wing vibration.

Fig. 2 shows a schematic configuration of the BWB airplane. In order to study aero-elastic and structural behavior utilizing finite element analysis, the main body is gridded into 6 beam elements and each wing is gridded into 4 beams. The control surfaces are located at the inner 3 elements of each wing, and they are labeled as input 1 to input 6. The \mathcal{H}_2 performance outputs are 3 nodal displacements at each wing element in z-direction, hence there are 24 nodal displacements in total. For example, outputs 1 and 12 are the nodal displacements at the right wing root and wing tip, respectively.

A general approach in developing an affine LPV model for an aero-elastic structure system can be described as follows: 1) A nonlinear aero-elastic model can be derived for a selected range of flight speeds [6]; 2) The nonlinear model is then linearized over gridded flight speeds to obtain a set of Linear Time Invariant (LTI) full-order models (FOMs); 3) A coordinate transformation is conducted to transfer the FOMs into modal coordinates; 4) Modal alignment and order-reduction [5] are performed to align modes for all LTI models and only the most significant modes over entire flight envelope are kept; 5) Linear interpolation over the aligned reduced-order models is operated to obtain the LPV model in affine form, as described in Eqn. (2).

The interpolation of aligned modes captures the variation of system dynamics as function of flight speed. It is important to note that if the models are not aligned, then a direct interpolation of system matrices will induce large modeling error [5]. In case of highly nonlinear behavior over a range of flight speeds, linear interpolation may need to be performed over multiple sub-regions to reduce modeling error, leading to the needs for switching LPV control design, which is a subject of our future research.

In this study, the selected range of scheduling parameter θ or flight speed is [110, 130] m/s, and a bundle of reduced-order LTI models are derived at varying flight speeds with an increment of 0.5 m/s to capture model variation. Six most dominant modes were chosen in the reduced-order LTI models, as marked by M1–M6 in Fig. 3. Physical meaning of each mode is described in Table 1. Note that all the bending/torsion coupling effects come from the backswept of the wing, and the wing structural rigidity itself has no inherent bending/torsion coupling. From Fig. 3, we can see that the (open-loop) eigenvalues vary with flight speed θ ,

Table 1
Mode description in reduced-order model.

Mode ID	Rigid-body component	Flexible component	Note
M1	Plunging and pitching	First symmetric out-of-plane bending	Bending/torsion coupling
M2	Plunging and pitching	Second symmetric out-of-plane bending	Bending/torsion coupling
M3	Plunging and pitching	First symmetric in-plane bending	Bending/torsion coupling
M4	Roll	Second anti-symmetric out-of-plane bending	Bending/torsion coupling
M5	–	First anti-symmetric in-plane bending	Bending/torsion coupling
M6	–	–	Aerodynamic dominant mode

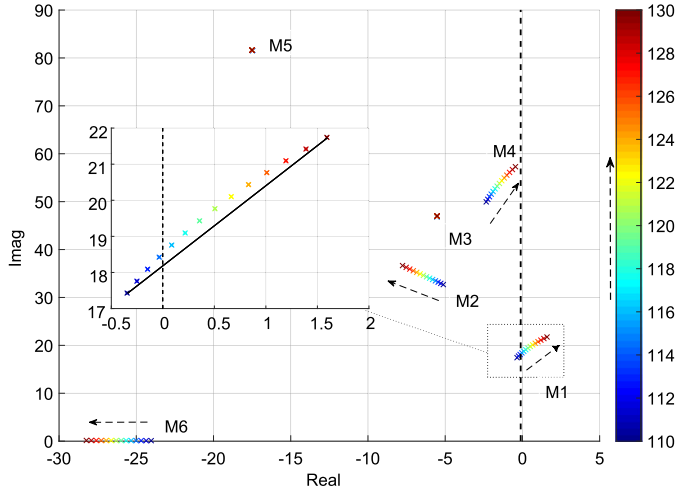


Fig. 3. Root loci of open-loop system. (For interpretation of the colors in the figure(s), the reader is referred to the web version of this article.)

and mode $M1$ becomes unstable when $\theta = 115$ m/s. The evolving directions of six modes associated with increasing flight speed are illustrated by the dashed arrow. The LPV model is obtained by linearly interpolating the first and last model, as shown in the close-up view of Fig. 3, where the solid line shows the linear interpolation of the eigenvalues, and the crosses denote the actual eigenvalue trajectory. Note that the interpolation error will be viewed as modeling error and handled by \mathcal{H}_∞ channel when formulating the robust ICC LPV control problem. Similarly, all other system matrices are also obtained by following the same linear interpolation process.

$$\Sigma(\theta) : \begin{bmatrix} \dot{x}(t) \\ z_\infty(t) \\ z_2(t) \end{bmatrix} = \begin{bmatrix} A_p(\theta(t)) & B_p(\theta(t)) & B_p(\theta(t)) & B_p(\theta(t)) \\ \begin{bmatrix} C_p(\theta(t)) \\ 0 \\ C_p(\theta(t)) \end{bmatrix} & \begin{bmatrix} D_p(\theta(t)) \\ 0 \\ 0 \end{bmatrix} & 0 & \begin{bmatrix} D_p(\theta(t)) \\ I \\ D_p(\theta(t)) \end{bmatrix} \end{bmatrix} \times \begin{bmatrix} x(t) \\ w_\infty(t) \\ w_2(t) \\ u(t) \end{bmatrix} \quad (31)$$

We study a scenario where the BWB airplane is subject to a sharp-edge gust disturbance, which then induces a constant shift angle on all control surfaces, more specifically we assume $w_2 = w_\infty = 0.005$ rad $\approx 0.28^\circ$. A gain-scheduling controller is designed to robustly suppress the bending displacement of the wing in the presence of gust disturbance. In this study, the hard constraints on flap deflection angles are imposed for two reasons: 1) available control authority is physically limited; 2) control inputs can not be too large in order to ensure the actuated dynamics are still within the linear range.

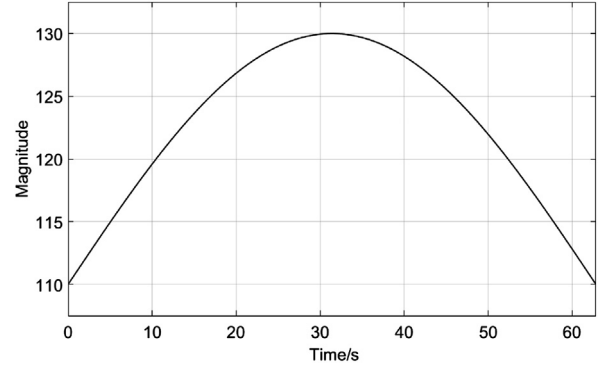


Fig. 4. Scheduling parameter (flight speed) trajectory.

The \mathcal{H}_2 outputs of interest are bending displacements, while the \mathcal{H}_∞ outputs include bending displacements and control inputs. Thus, by following the procedures described above, the LPV system description can be derived as in (31). The weighting matrix Q is chosen to be an identity, that is, all outputs are weighted equally. The scheduling parameter is chosen as a biased sinusoidal function, $\theta(t) = 110 + 20 \sin(t/20)$ m/s, as shown in Fig. 4. Therefore, within the time interval of $[0, 20\pi]$ second, the scheduling parameter is bounded as $110 \text{ m/s} \leq \theta \leq 130 \text{ m/s}$, and its rate bounded as $-1 \text{ m/s}^2 \leq \dot{\theta} \leq 1 \text{ m/s}^2$. In general, the scheduling parameter trajectory should satisfy the boundary conditions for both θ and $\dot{\theta}$, and be at least piece-wise differentiable. It is commonly accepted that the variation of the scheduling parameters must be ‘slow’ compared to the system dynamics, because designing an LPV controller for fast-varying scheduling parameters is a challenge [34].

5.1. Constraints and performance trade-off

In the mixed ICC and \mathcal{H}_∞ (or robust ICC) LPV control problem, both control input constraints and robustness requirement would significantly impact the optimal solution to the PLMIs. Hence, a trade-off study is conducted to better understand the characteristics of LPV models. Fig. 5 shows the complete trade-off between the control effort \bar{U} , the robustness levels γ_∞ , and the output performance $\text{trace}(W)$. For a given robustness level, the trade-off contour illustrates that larger control input constraint leads to smaller output covariance, hence better \mathcal{H}_2 performance for the closed-loop system. In addition, with small control effort, output performance will be degraded, resulting in a large output covariance. An increase in control effort leads to notable improvement on system \mathcal{H}_2 performance with wider range of admissible robustness levels. This demonstrates that larger control input can effectively compensate for the robustness constraints.

Furthermore, based on the Small Gain Theorem [25], the closed-loop system satisfying the condition $\|T_\infty\|_\infty \leq \gamma_\infty$ is well-posed and internally stable for all uncertainty satisfying $\|\Delta\|_\infty < 1/\gamma_\infty$, where Δ can be considered as an interconnection from z_∞ to w_∞ , as was shown in Fig. 1. In Fig. 5, with a fixed \bar{U} , it is obvious that with more stringent requirement on robust performance, i.e. smaller γ_∞ , the output performance degrades with increase in

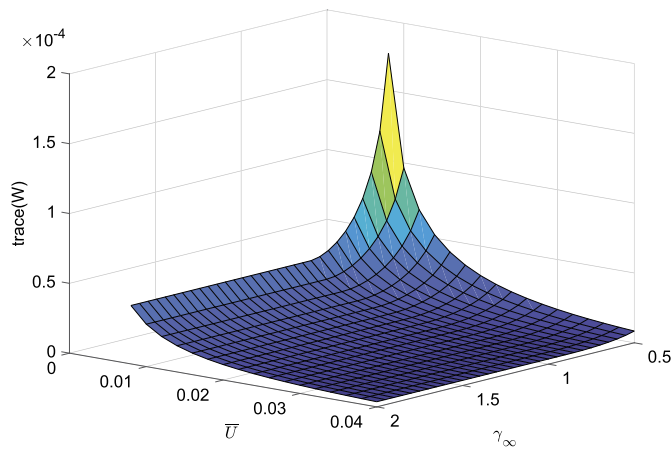


Fig. 5. Trade-off between control limit \bar{U} and $\text{trace}(W)$ at different robustness conditions.

$\text{trace}(W)$, leading to worsen \mathcal{H}_2 performance. Note that, while γ_∞ decreases incrementally, $\text{trace}(W)$ increases or \mathcal{H}_2 performance degrades much drastically. This can be explained by the reciprocal relation between uncertainty Δ and γ_∞ .

The trend at higher or lower robustness level reveals an important implication for controller design. At lower robustness level, for instance $\gamma_\infty = 2$, the \mathcal{H}_2 performance remains almost unchanged when $\bar{U} > 0.01$. This indicates that the robust \mathcal{H}_∞ performance requirement is not the dominant factor for control design and the \mathcal{H}_2 performance can be achieved with a relatively small control effort. However, at higher robustness level, for instance $\gamma_\infty = 0.5$, the \mathcal{H}_∞ performance becomes critical for control design. As a result, in order to achieve a specific \mathcal{H}_2 performance, more control effort is required. It is also observed that the achievable \mathcal{H}_2 performance degrades with increase in robustness level. Based on the above-mentioned trade-offs, the constraints for the control design are chosen to be $\bar{U} = 0.02$ and $\gamma_\infty = 1$, which ensure a good robustness margin to handle modeling error while balancing between \mathcal{H}_2 performance and control effort.

5.2. Time domain simulation results

Given the range of θ and $\dot{\theta}$, the control input constraints, and the robustness level, the LPV model of BWB airplane is simulated when it is subjected to a sharp-edged gust disturbance for 5 seconds. Figs. 6 and 7 show the wing root (output 1) and wing tip (output 12) bending displacement of the right wing for open-loop case, and as can be seen the results are unstable. Therefore, a state-feedback LPV controller in the form of Eqn. (4) is designed to stabilize wing elements and suppress the bending displacement.

Using Theorem 1, a state-feedback LPV controller can be design with scheduled control gain matrix of dimension 6×12 , mapping 12 states to 6 control inputs. Note that the LPV model is developed in the modal coordinate, the measured or observed states in original coordinate need to be transformed to the modal coordinate. In practical implementation, scheduling parameter (flight speed) will be online measured in each sampling time, and control inputs of altering flap angles can be calculated from corresponding controller gain matrix and measured or observed states.

To demonstrate the effect of control input constraints and robustness levels to \mathcal{H}_2 performance, multiple simulations are performed for comparison. When robustness level $\gamma_\infty = 1$ is fixed, each control input is identically constrained by various upper bounds \bar{U} . Figs. 8 and 9 show the bending displacement at wing root and wing tip for $\bar{U} = 0.01, 0.02, 0.04$. As can be seen, during the gust disturbance, the outputs are converged and bounded. In addition, with larger control inputs, the output responses have

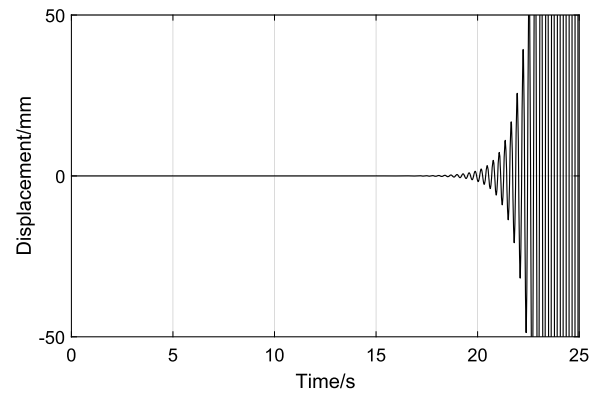


Fig. 6. Bending displacement at wing root.

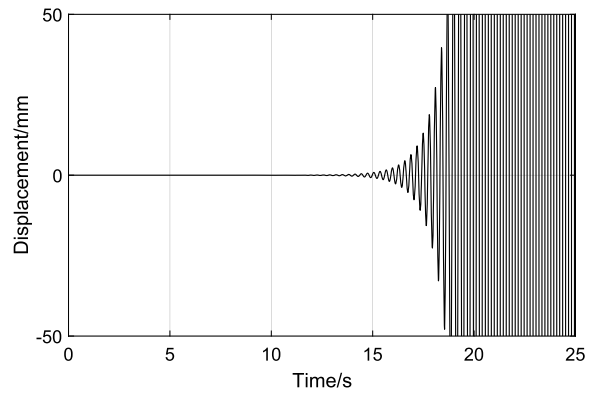


Fig. 7. Bending displacement at wing tip.

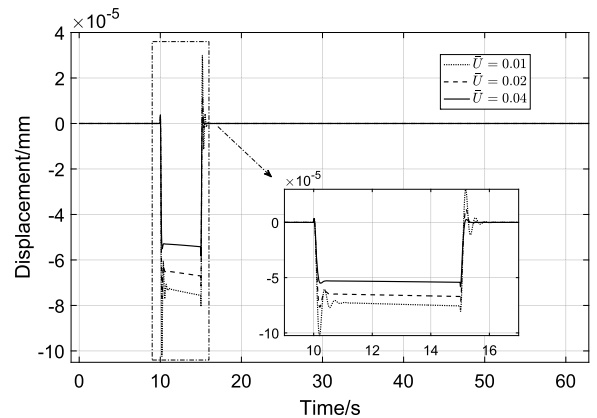


Fig. 8. Wing root bending under different \bar{U} .

smaller overshoot and faster convergent rate, indicating that \mathcal{H}_2 output performance are improved. As shown in Figs. 10–15, the control inputs 1–6 are increased by more than twice when upper bounds become doubled. This comparison indicates that the selection of $\bar{U} = 0.02$ offers a good balance between the performance and the control effort, which produces an upper bound of $u = 0.14 \text{ rad} \approx 8^\circ$.

All 6 inputs are compared to show how the control law allocates 6 independent inputs to suppress airplane wing displacements. It can be observed that inputs 1 and 3 are distributed by similar control authority. The equal distribution of control authority also happens on control inputs 2 and 4, control inputs 5 and 6.

When $\bar{U} = 0.02$ is fixed, the robustness level γ_∞ is varied to study its influence on output performance. As shown in Figs. 16 and 17, the bending displacement at wing root and wing tip are

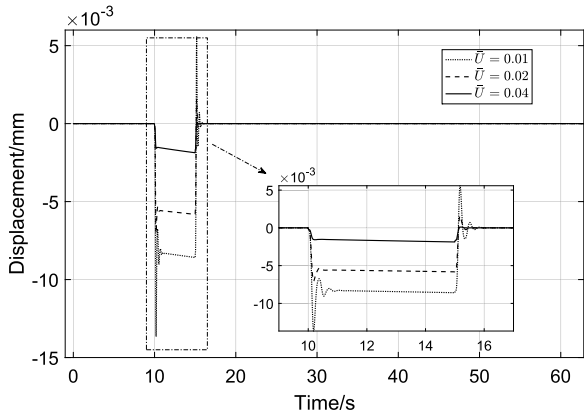


Fig. 9. Wing tip bending under different \bar{U} .

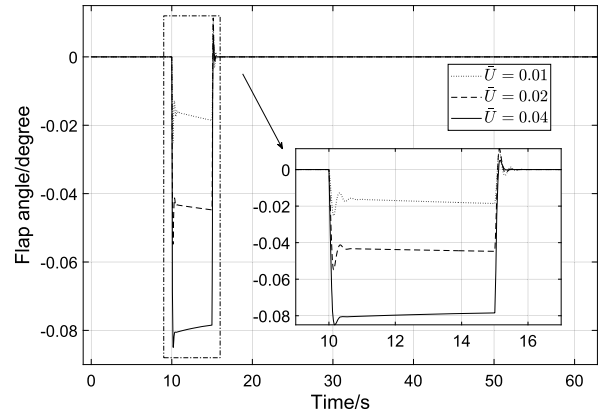


Fig. 12. Control input 3 under different \bar{U} .

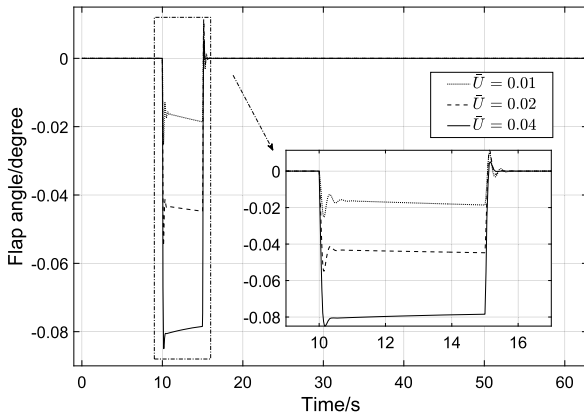


Fig. 10. Control input 1 under different \bar{U} .

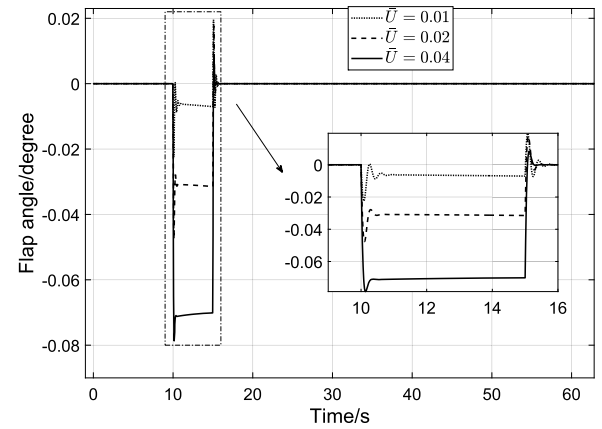


Fig. 13. Control input 4 under different \bar{U} .

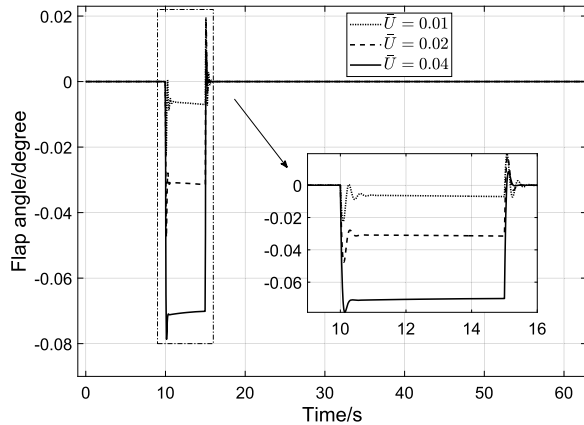


Fig. 11. Control input 2 under different \bar{U} .

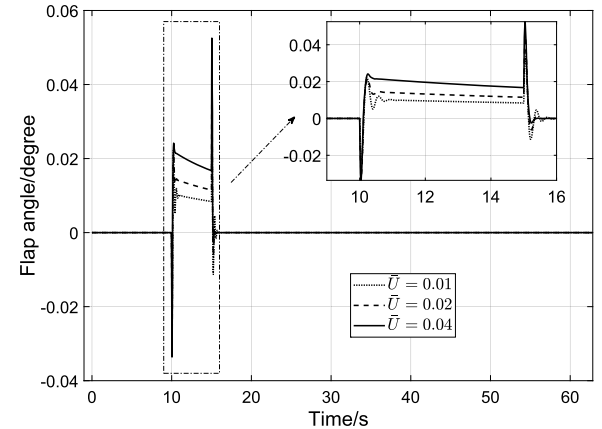


Fig. 14. Control input 5 under different \bar{U} .

improved when γ_∞ increases from 0.5 to 1. However, the responses remain almost unchanged when γ_∞ increases from 1 to 2. This phenomenon matches well with the earlier trade-off study shown in Fig. 5. Figs. 18–23 show the control inputs when the robustness level is greater than 1, as can be seen that γ_∞ is no longer the dominant factor for output performance.

After \bar{U} is chosen, LPV controller is designed and applied to actual gridded LTI models to validate its feasibility. Fig. 24 shows the root loci of the closed-loop system with varying flight speed. As shown, the proposed LPV controller stabilizes the gridded LTI models subject to input constraints, while minimizing the output \mathcal{H}_2 performance. However, in an effort to reduce control energy, some modes are kept unchanged by proposed controller.

Comparing Figs. 3 and 24, the modes ($M1, M2, M4$), dominating z-directional bending motion, have been significantly shifted, while other modes ($M3, M5, M6$) are kept unchanged. In addition, Fig. 25 shows the ICC cost or \mathcal{H}_2 norm of the closed-loop system with LPV controller applied to interpolated LPV system and actual gridded LTI models, respectively. Their magnitudes are very close and upper bounded by $trace(W)$. When combining with Fig. 24, Fig. 25 effectively validates that the proposed interpolation of LTI models and LPV controller design is feasible for vibration control of BWB airplane.

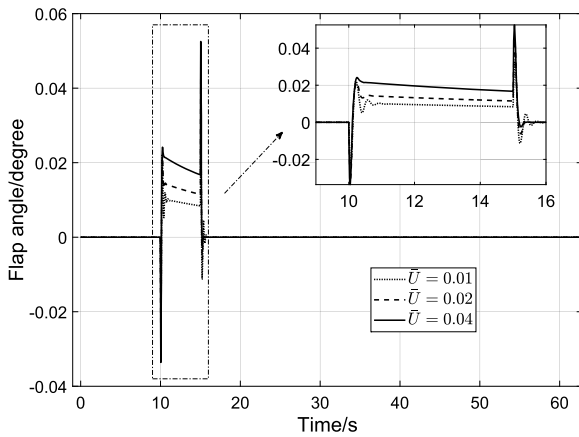


Fig. 15. Control input 6 under different \bar{U} .

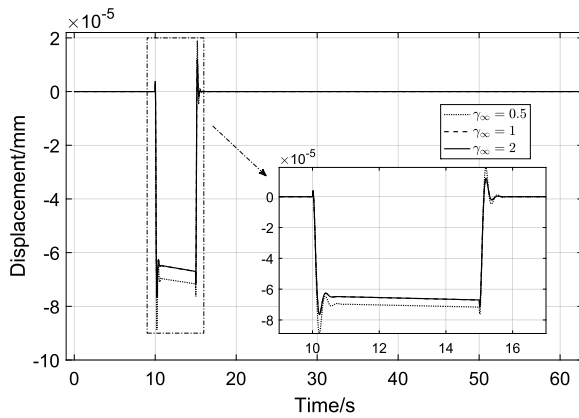


Fig. 16. Wing root bending under different γ_∞ .

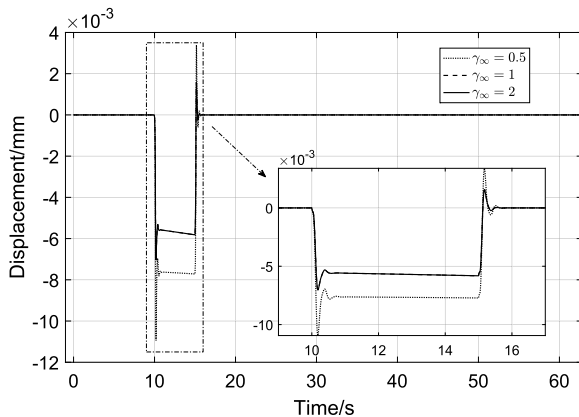


Fig. 17. Wing tip bending under different γ_∞ .

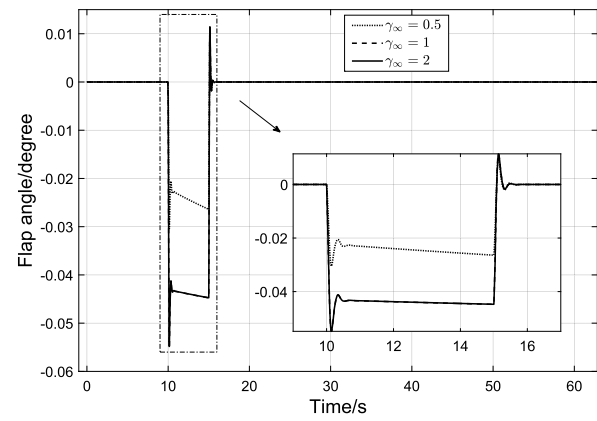


Fig. 18. Control input 1 under different γ_∞ .

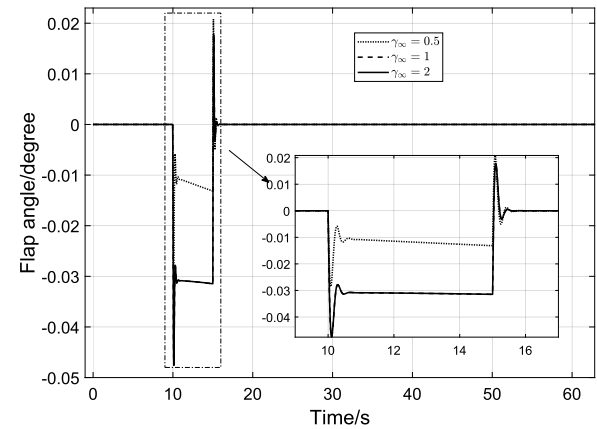


Fig. 19. Control input 2 under different γ_∞ .

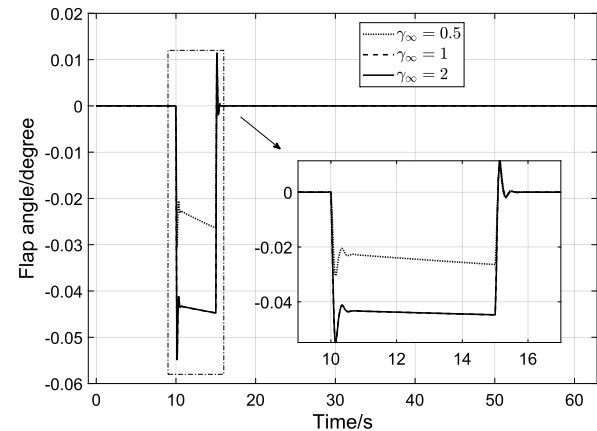


Fig. 20. Control input 3 under different γ_∞ .

6. Conclusion

The mixed ICC and \mathcal{H}_∞ control problem was proposed and the associated synthesis PLMI conditions were developed for designing the optimal controllers via convex optimization. The mixed ICC and \mathcal{H}_∞ controller minimizes \mathcal{H}_2 output covariance performance subject to multiple constraints on the control input and robust \mathcal{H}_∞ performance requirements. The proposed LPV control design scheme was applied to the BWB airplane model for vibration suppression. A comprehensive design trade-offs were studied, including the input covariance, output covariance, and robustness. The trade-offs provided an insight into how these constraints influence the closed-loop system performance. Simulations were conducted

for different control bounds, and the results demonstrated that the proposed LPV controller was able to exponentially stabilize the closed-loop system, while enhancing the output performance with faster convergence and reduced oscillation. It was shown that for a given \mathcal{H}_∞ norm bound, the output performance improves as the available control effort increases, and for a given control effort, the system performance improves as the \mathcal{H}_∞ norm bound is reduced. Furthermore, the proposed approach would provide a family of LPV controllers with varying control gains that could be tailored for LPV control systems to achieve optimal performance.

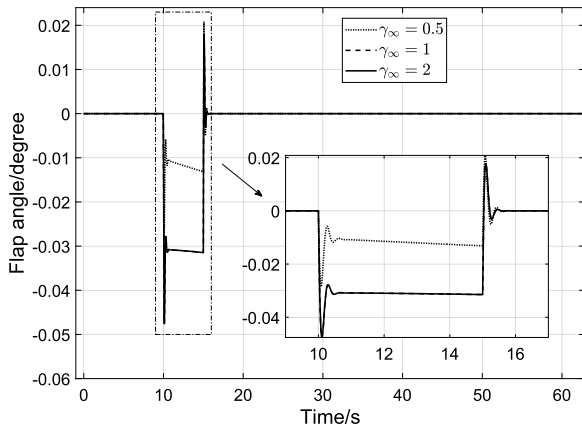


Fig. 21. Control input 4 under different γ_∞ .

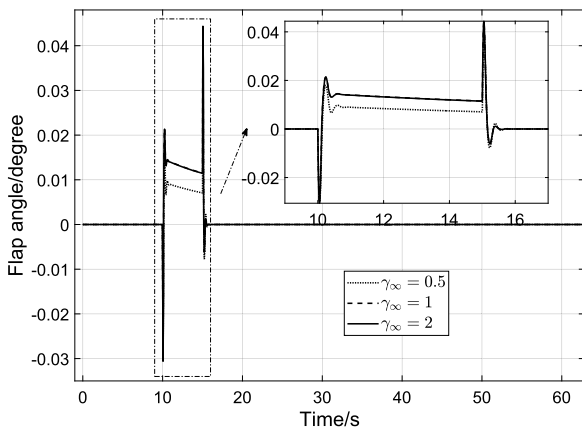


Fig. 22. Control input 5 under different γ_∞ .

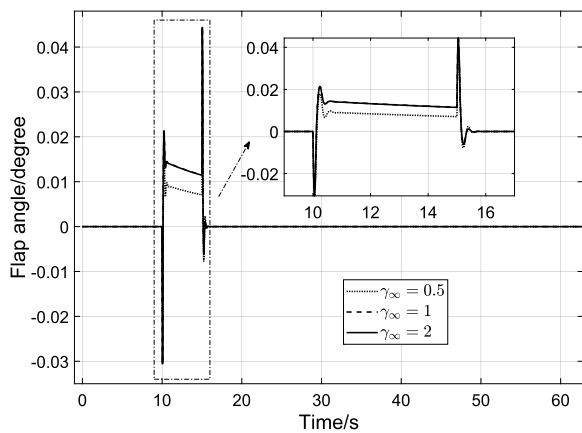


Fig. 23. Control input 6 under different γ_∞ .

Conflict of interest statement

The authors declare that there is no conflict of interest.

Acknowledgements

This research is supported by NASA ARMD Convergent Aeronautics Solutions (CAS) Project under funding number NNX15AR80G.

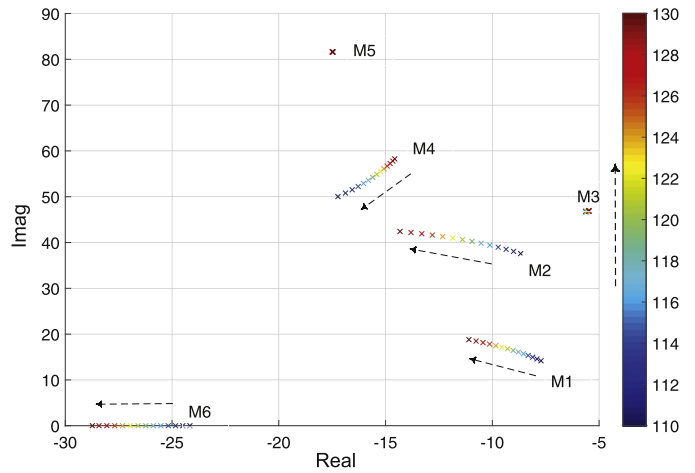


Fig. 24. Root loci of closed-loop system.

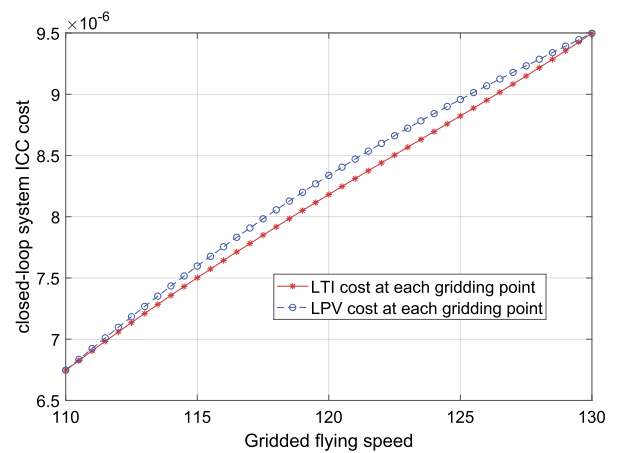


Fig. 25. Closed-loop ICC cost with LPV and LTI models.

References

- [1] G. Becker, A. Packard, Robust performance of linear parametrically varying systems using parametrically-dependent linear feedback, *Syst. Control Lett.* 23 (3) (1994) 205–215.
- [2] P. Apkarian, P. Gahinet, G. Becker, Self-scheduled \mathcal{H}_∞ control of linear parameter-varying systems: a design example, *Automatica* 31 (9) (1995) 1251–1261.
- [3] A. White, G. Zhu, J. Choi, *Linear Parameter-Varying Control for Engineering Applications*, Springer, London, 2013.
- [4] W.J. Rugh, J.S. Shamma, Research on gain scheduling, *Automatica* 36 (10) (Oct. 2000) 1401–1425.
- [5] A. Al-jiboory, G. Zhu, S.S.-M. Sweil, W. Su, N.T. Nguyen, LPV modeling of a flexible wing aircraft using adaptive model gridding and alignment methods, *Aerosp. Sci. Technol.* 66 (July 2017) 92–102.
- [6] W. Su, C.E.S. Cesnik, Nonlinear aeroelasticity of a very flexible blended-wing-body aircraft, *J. Aircr.* 47 (5) (Sep. 2010) 1539–1553.
- [7] P. Apkarian, H.D. Tuan, J. Bernussou, Continuous-time analysis, eigenstructure assignment, and \mathcal{H}_2 synthesis with enhanced linear matrix inequalities (LMI) characterizations, *IEEE Trans. Autom. Control* 46 (12) (2001) 1941–1946.
- [8] R.C.L.F. Oliveira, P.L.D. Peres, Parameter-dependent LMIs in robust analysis: characterization of homogeneous polynomially parameter-dependent solutions via LMI relaxations, *IEEE Trans. Autom. Control* 52 (7) (July 2007) 1334–1340.
- [9] W. Xie, \mathcal{H}_2 gain scheduled state feedback for LPV system with new LMI formulation, *IEE Proc., Control Theory Appl.* 152 (6) (Nov. 2005) 693–697.
- [10] P. Apkarian, P. Gahinet, A convex characterization of gain-scheduled \mathcal{H}_∞ controllers, *IEEE Trans. Autom. Control* 40 (5) (1995) 853–864.
- [11] F. Wu, X.H. Yang, A. Packard, G. Becker, Induced \mathcal{L}_2 norm control for LPV systems with bounded parameter variation rates, *Int. J. Robust Nonlinear Control* 6 (9–10) (1996) 983–998.
- [12] J. Swevers, Gain-scheduled \mathcal{H}_2 and \mathcal{H}_∞ control of discrete-time polytopic time-varying systems, *IET Control Theory Appl.* 4 (3) (Mar. 2010) 362–380.
- [13] G. Zhu, K.M. Grigoriadis, R.E. Skelton, Covariance control design for Hubble Space Telescope, *J. Guid. Control Dyn.* 18 (2) (Mar. 1995) 230–236.

- [14] A. Hotz, R.E. Skelton, Covariance control theory, *Int. J. Control* 46 (1) (1987) 13–32.
- [15] G. Zhu, L-2 and L-Infinity Multiobjective Control for Linear Systems, Ph.D. thesis, Purdue University, West Lafayette, 1992.
- [16] C. Hsieh, R.E. Skelton, F.M. Damra, Minimum energy controllers with inequality constraints on output variances, *Optim. Control Appl. Methods* 10 (4) (1989) 347–366.
- [17] G. Zhu, M. Rotea, R.E. Skelton, A convergent algorithm for the output covariance constraint control problem, *SIAM J. Control Optim.* 35 (1) (Jan. 1997) 341–361.
- [18] A. Al-Jiboory, A. White, S. Zhang, G. Zhu, J. Choi, Linear matrix inequalities approach to input covariance constraint control with application to electronic throttle, *J. Dyn. Syst. Meas. Control* 137 (9) (2015) 091010.
- [19] A. Al-Jiboory, G. Zhu, C. Sultan, LMI control design with input covariance constraint for a tensegrity simplex structure, in: *ASME Dynamic Systems and Control Conference*, Oct. 2014, V003T52A004.
- [20] C. Scherer, Mixed $\mathcal{H}_2/\mathcal{H}_\infty$ control for time-varying and linear parametrically-varying systems, *Int. J. Robust Nonlinear Control* 6 (9–10) (Nov. 1996) 929–952.
- [21] C. Scherer, P. Gahinet, M. Chilali, Multi-objective output-feedback control via LMI optimization, *IEEE Trans. Autom. Control* 42 (7) (1997) 896–911.
- [22] P. Apkarian, P.C. Pellanda, H.D. Tuan, Mixed $\mathcal{H}_2/\mathcal{H}_\infty$ multi-channel linear parameter-varying control in discrete time, *Syst. Control Lett.* 41 (5) (Dec. 2000) 333–346.
- [23] A. White, G. Zhu, J. Choi, Optimal LPV control with hard constraints, *Int. J. Control. Autom. Syst.* 14 (1) (2016) 148–162.
- [24] S. Zhang, J. Yang, G. Zhu, LPV modeling and mixed constrained $\mathcal{H}_2/\mathcal{H}_\infty$ control of an electronic throttle, *IEEE/ASME Trans. Mechatron.* 20 (5) (2015) 2120–2132.
- [25] K. Zhou, J.C. Doyle, K. Glover, *Robust and Optimal Control*, Prentice-Hall, Inc., Upper Saddle River, NJ, USA, 1996.
- [26] R.E. Skelton, T. Iwasaki, K. Grigoriadis, *A Unified Algebraic Approach to Linear Control Design*, Taylor & Francis Ltd., London, UK, 1998.
- [27] M.J. Lacerda, E.S. Tognetti, R.C.L.F. Oliveira, P.L.D. Peres, A new approach to handle additive and multiplicative uncertainties in the measurement for \mathcal{H}_∞ LPV filtering, *Int. J. Syst. Sci.* 47 (5) (2016) 1042–1053.
- [28] R.C.L.F. Oliveira, P. Bliman, P.L.D. Peres, Robust LMIs with parameters in multi-simplex: existence of solutions and applications, in: *47th IEEE Conference on Decision and Control*, Dec. 2008, pp. 2226–2231.
- [29] G. Pipeleers, B. Demeulenaere, J. Swevers, L. Vandenberghe, Extended LMI characterizations for stability and performance of linear systems, *Syst. Control Lett.* 58 (7) (2009) 510–518.
- [30] C. Scherer, LMI relaxations in robust control, *Eur. J. Control* 12 (1) (2006) 3–29.
- [31] C.M. Agulhari, R.C.L.F. Oliveira, P.L.D. Peres, Robust LMI parser: a computational package to construct LMI conditions for uncertain systems, in: *XIX Brazilian Conference on Automation, CBA 2012, Campina Grande, PB, Brazil, 2012*, pp. 2298–2305.
- [32] J. Löfberg, YALMIP: a toolbox for modeling and optimization in MATLAB, in: *Proceedings of the CACSD Conference, Taipei, Taiwan, Sep. 2004*, pp. 284–289.
- [33] J. Sturm, Using SeDuMi 1.02, a MATLAB toolbox for optimization over symmetric cones, *Optim. Methods Softw.* 11 (1) (1999) 625–653.
- [34] J.S. Shamma, An overview of LPV systems, in: J. Mohammadpour, C.W. Scherer (Eds.), *Control of Linear Parameter Varying Systems with Applications*, Springer US, Boston, MA, 2012, pp. 3–26.